Activating [4+4] photoreactivity in the solid-state via complexation: from 9-(methylaminomethyl)anthracene to its silver(I) complexes.

Floriana Spinelli, Simone d' Agostino, Paola Taddei, Christopher D. Jones, Jonathan W. Steed and Fabrizia Grepioni

Electronic Supplementary Information

(16 pages)

Contents

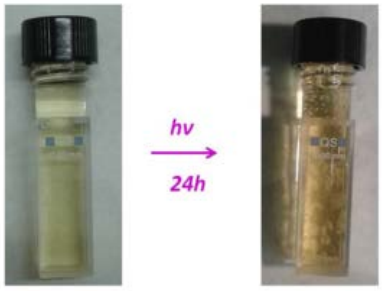

Fig. S1 Crystallization of the trans photodimer, DMAMA, after irradiation at λ = 365 nm of a saturated ethanolic solution.

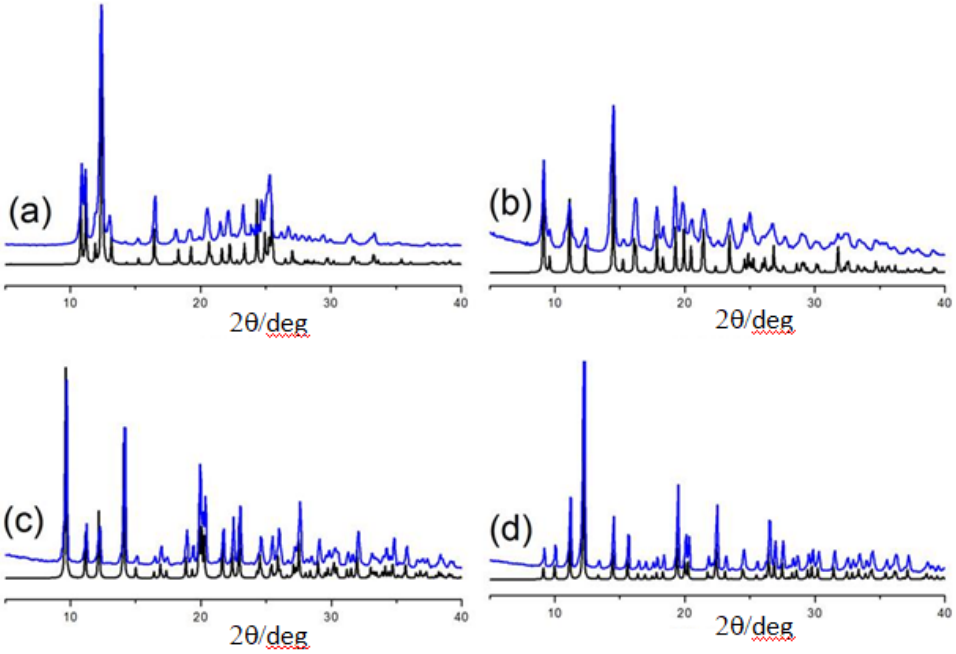

Fig. S2 Experimental (blue line) and simulated (black line) X-ray powder diffraction patterns for (a) DMAMA and for the complexes (b) $[Ag(MAMA)_2][PF_6]$, (c) $[Ag(MAMA)_2][BF_4]$ and (d) $[Ag(MAMA)_2][Ag(NO_3)_2]$.

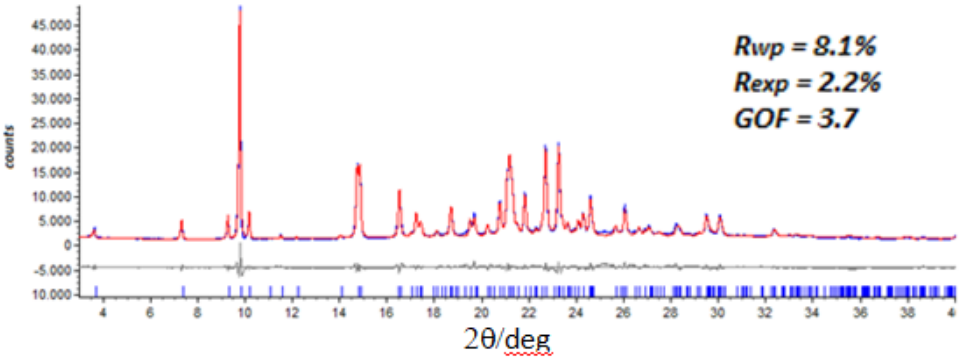

Fig. S3 Experimental (blue), calculated (red) and difference (grey) patterns for the free ligand MAMA.

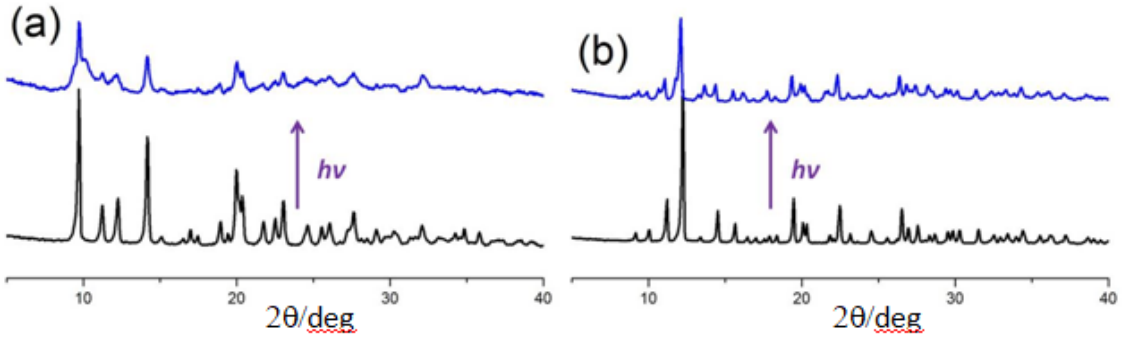

Fig. S4 Comparison between experimental X-ray powder diffraction patterns run before (black line) and after (blue line) UV irradiation for the complexes: (a) $[Ag(MAMA)_2][BF_4]$ and (b) $[Ag(MAMA)_2][Ag(NO_3)_2]$.

Table S1 Crystal data and details of measurements for crystalline MAMA, DMAMA, $Ag(MAMA)_2[PF_6]$, $Ag(MAMA)_2[BF_4]$, $[Ag(MAMA)_2][Ag(NO_3)_2]$, and $[DMAMAH_2]Br_2$.

	MAMA	**DMAMA**	**$[Ag(MAMA)_2][PF_6]$**	**$[Ag(MAMA)_2][BF_4]$**	**$[Ag(MAMA)_2][Ag(NO_3)_2]$**	**$[DMAMAH_2]Br_2$**
Formula	$C_{15}H_{16}N$	$C_{16}H_{15}N$	$C_{32}H_{30}AgF_6NP$	$C_{32}H_{30}AgBF_4N$	$C_{16}H_{15}AgN_2O_3$	$C_{32}H_{32}Br_2N_2$
Fw (g/mol)	221.30	221.29	695.42	637.28	391.17	604.42
Cryst. System	Triclinic	Triclinic	Monoclinic	Monoclinic	Monoclinic	Monoclinic
Space group	P-1	P-1	C2/c	C2/c	C2/c	$P2_1/n$
Z	2	2	8	8	8	4
Z'	2	2 x 0.5	0.5	0.5	0.5	0.5
a (Å)	24.1250(1)	8.1706(5)	19.4884(9)	18.6597(9)	20.4242(12)	9.202(5)
b (Å)	9.65362(3)	9.2479(6)	10.4542(4)	10.2048(4)	8.1480(4)	7.953(5)
c (Å)	5.48188(2)	16.4024(10)	14.4045(9)	14.7676(8)	18.6493(13)	18.223(5)
α (deg)	100.5596(4)	92.8970(10)	90	90	90	90
β (deg)	96.2248(5)	93.1560(10)	96.753(5)	100.540(5)	108.776(7)	93.342(5)
γ (deg)	85.6998(3)	110.3720(10)	90	90	90	90
V (Å^3)	1245.69(5)	1156.88(13)	2914.3(3)	2764.6(2)	2938.4(3)	1331.4(12)
D_{calc} (g/cm^3)	1.180	1.271	1.585	1.531	1.768	1.508
μ (mm^{-1})	-	0.074	0.810	0.781	1.386	3.069
Measd reflns	-	18826	7545	6336	7363	5040
Indep reflns	-	6729	3379	3140	3375	2348
R_1(obs)	-	0.0555	0.083	0.0602	0.0786	0.0740
wR_2 (all data)	-	0.1639	0.204	0.222	0.1626	0.1003
R_{wp}	8.2	-	-	-	-	-
R_{exp}	2.1	-	-	-	-	-

Gel Phase Crystallization

LMWGs have been successfully used as media for crystal growth. The intrinsic supramolecular nature of such systems is potentially useful since their formation/disruption displays reversibility upon the application of a suitable stimulus, which can be used for the easy recovery of the gel-grown crystals. In order to test the photoreactivity of anthracene in a gel of bis(urea) gelator G1, both anthracene and the gelator were dissolved in toluene, and, after heating, the gel was obtained. After an overnight irradiation of the gel at λ = 365 nm crystals were obtained, which were recovered after gel decomposition with an ethanolic solution of tetrabutylammonium acetate, and subsequently tested by X-ray single crystal diffraction (see Fig. S5). The unit cell of the crystals corresponded to the unit cell of the anthracene dimer reported in the CSD. A comparison between crystals of the dianthracene obtained via solution irradiation and those obtained from gel showed that crystals grown in the gel medium are much larger with respect to those grown in solution (Fig. S6).

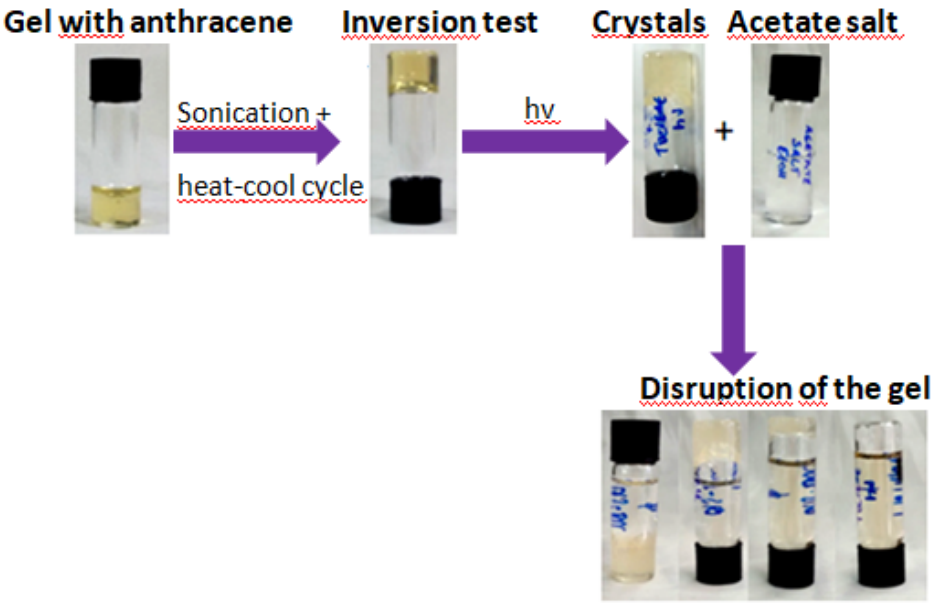

Fig. S5a Irradiation of anthracene in gel medium and subsequent gel disruption using an ethanolic solution of tetrabutylammonium acetate.

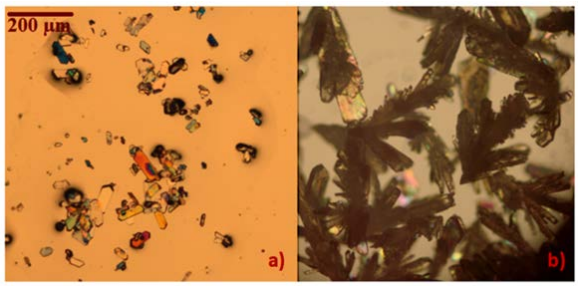

Fig. S5b Pictures of the crystals of dianthracene obtained after irradiation in solution (left) and in the gel medium (right), taken by optical microscope.

^{1}H NMR spectroscopy

Solution ^{1}H NMR spectroscopy was also employed to follow the cyclization reaction in the gel for both anthracene and MAMA. Figure S6a shows how the intensity of the aromatic CH signals decreases upon increasing the irradiation time, while signals corresponding to the tertiary bridgehead aliphatic CH protons start to appear (however they immediately disappear again due to precipitation of the anthracene dimer, which is insoluble in the gel). In the case of MAMA (see Fig. S6b), which is only slightly soluble in toluene, no crystal formation was observed, although the NMR spectra show - as in the case of anthracene - a decrease in the intensity of the aromatic CH signals and, after a much longer time, the appearance of resonances assigned to bridgehead aliphatic CH protons. Interaction of MAMA with gel fibres, together with its low concentration, might be the reason why formation of the photocyclization product could only be detected after a long time, and no crystal growth could be observed.

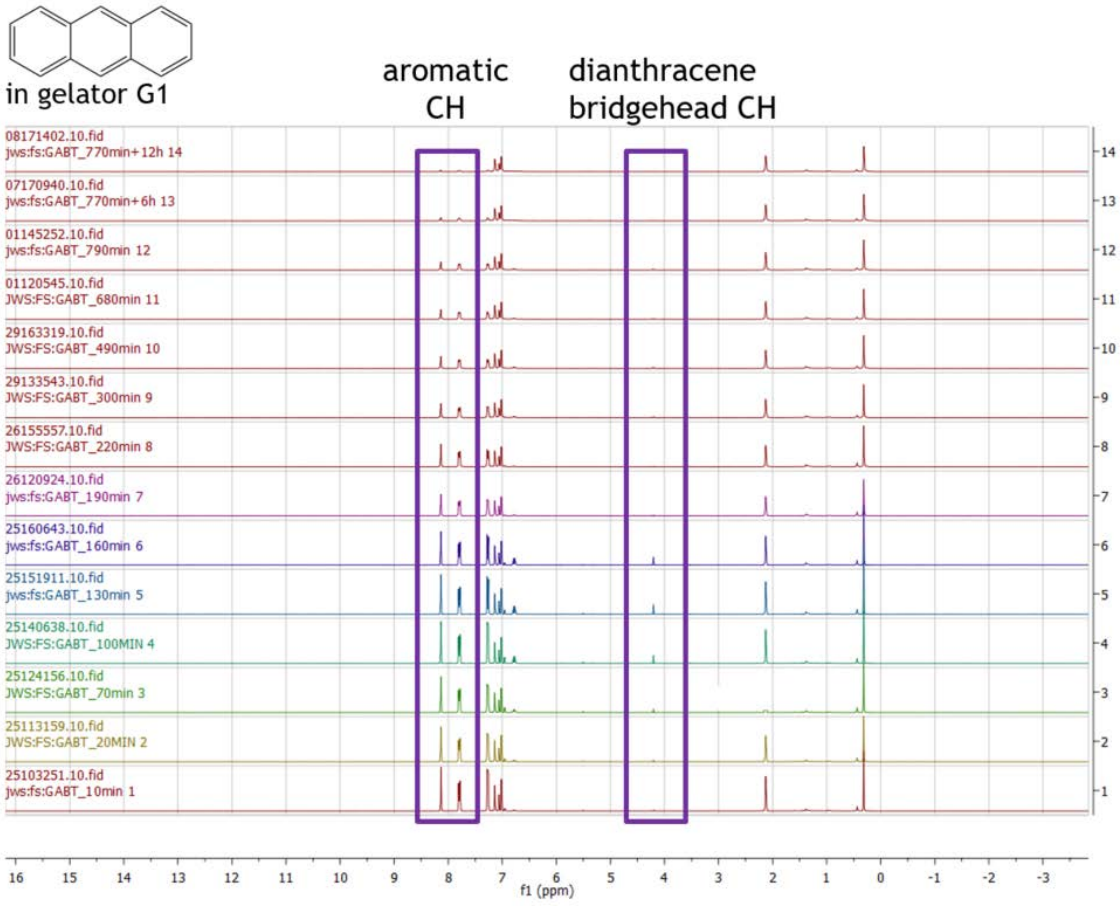

Fig. S6a Solution ^{1}H NMR spectra of anthracene in gel: the intensity of the aromatic CH signals decreases upon increasing the irradiation time, while signals corresponding to the tertiary bridgehead aliphatic CH start to appear after a few minutes (however they immediately disappear again due to precipitation of the anthracene dimer, which is insoluble in the gel).

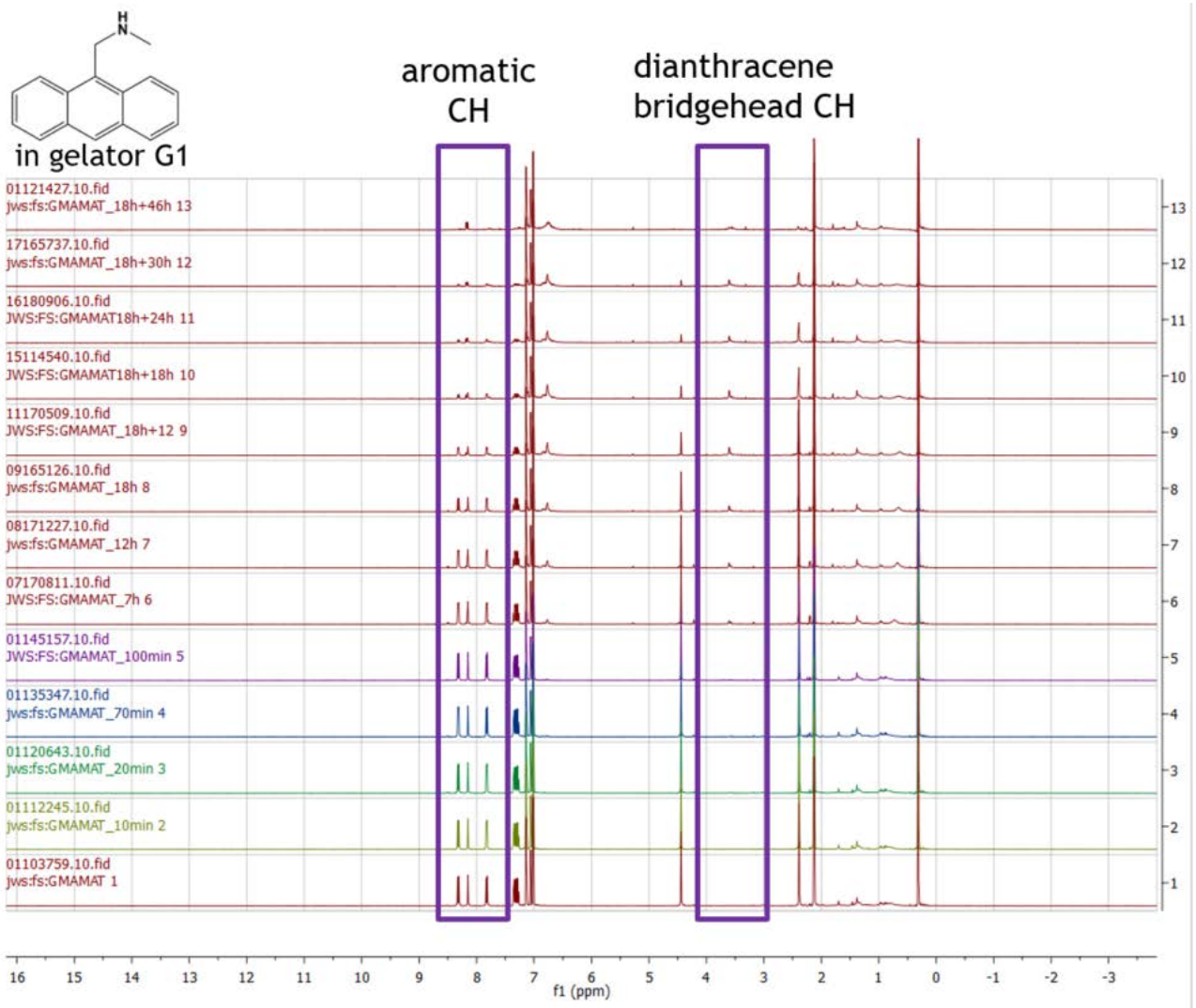

Fig. S6b Solution ^{1}H NMR spectra of MAMA in gel: the intensity of the aromatic CH signals decreases upon increasing the irradiation time, while signals corresponding to the tertiary bridgehead aliphatic CH start to appear only after many hours.

Synthesis of the gelator G1

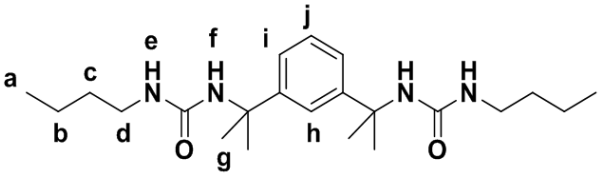

To a stirred solution of *n*-butylamine (0.1 cm^3, 1.01 mmol) in chloroform (20 cm^3) at 20 ºC was added 1,3-bis(1-isocyanato-1-methylethyl)benzene (0.1 cm^3, 0.43 mmol). The reaction mixture was left to stand under air for 24 hours at 20 ºC then concentrated *in vacuo* and filtered under suction. The collected solids were washed with chloroform (2 x 20 cm^3) and dried in a drying pistol. Compound **1** was obtained as a white solid (152 mg, 0.39 mmol, 90%), m/z (ESI-MS) 413.8 $[M+Na]^+$. ^{1}H NMR (400 MHz, DMSO-d_6) δ 7.33 (t, J = 1.8 Hz, 1H, *h*), 7.20 – 7.08 (m, 3H, *i*, *j*), 6.12 (s, 2H, *f*), 5.75 (t, J = 5.7 Hz, 2H, *e*), 2.92 (dt, J = 6.3, 5.7 Hz, 4H, *d*), 1.51 (s, 12H, *g*), 1.38 – 1.18 (m, 8H, *b*, *c*), 0.95 – 0.73 (m, 6H, *a*). ^{13}C NMR (101 MHz, DMSO-d_6) δ 157.59, 148.97, 127.68, 122.75, 121.75, 54.65, 38.96, 32.71, 30.63, 19.99, 14.17. Anal. Calc. (%) ($C_{22}H_{38}N_4O_2$) C 67.66, H 9.81, N 14.35; Found (%) C 67.40, H 9.72, N 14.27.

Raman spectroscopy

Table S2 Main Raman band wavenumbers and assignments for MAMA and DMAMA. The band wavenumbers of dianthracene are reported for comparison. The bands characteristic of fused benzene rings are highlighted in bold. The bands characteristic of the dimer are indicated in red.

Assignments	**MAMA**	**DMAMA**	**Dianthracene[1]**	**Assignments**
CC ring stretching in anthracene[2,3], in alkyl-substituted anthracenes[4], and 9-substituted derivatives[5,6]	1625 vw			
		1597-1591 m	1603-1592	Phenyl CC stretching in 9,10-dihydroanthracene[7] and ortho-xylene[8,9]
CC ring stretching in anthracene and 9-substituted derivatives[2,3,5]	1575 sh	1576 sh	1582	Phenyl CC stretching in dianthracene[1] and 9,10-dihydroanthracene[7]
CC ring stretching in anthracene and 9-substituted derivatives[2,3,5,6]	1558 s			
Aromatic CH in plane bending[5] and CC ring stretching[6] in anthracene[10] and	1503-1493 w			

9-substituted derivatives				
CC ring stretching in anthracene and 9-substituted derivatives[2,5], aromatic CH in plane bending in anthracene[3, 5]	1477 m	1479 mw	1464	Phenyl CC stretching in 9,10-dihydroanthracene[7]
CH_3 symmetric deformation[8]	1453 w	1453 w		
CC ring stretching in antharacene[2,3,5] and 9-substituted anthracene[8,11] **characteristic of fused benzene rings[12]**	**1408 vs**	1410 w		
Aromatic CH in plane bending in anthracene[3,5] CC ring stretching in 9-substituted anthracene[6,8,11], CH_3 antisymmetric deformation[6,8]	1381 m			
Aromatic CH in plane bending in anthracene and 9-substituted anthracene[5]	1356 ms			
		1348 vw	1338	Tertiary CH deformation[8]
Aromatic CH in plane bending in anthracene[3,5]	1278 m	1271 vw	1265	CH in plane bending in 9,10-dihydroanthracene[7]
CC ring stretching[2,3] and aromatic CH in plane bending[5] in anthracene	1258 m	1261 sh	1263	CH out of phase bending in 9,10-dihydroanthracene[7]
		1211 vs	1228	CC symmetric stretching in 9,10-dihydroanthracene[7], ortho-dialkylbenzenes[8,9]
		1194 sh br	1187	CC antisymmetric stretching in 9,10-dihydroanthracene[7], internal quaternary carbon atom[8]
CH in plane bending in anthracene[2,3,5]	1181 m		1178	
		1167 mw	1158	Internal tertiary carbon atom[8]
CH in plane bending in anthracene and 9-substituted anthracene[3,5,6], aliphatic CH bending[6,8]	1155-1142 vw	1153-1141 vw		
Aromatic CH in plane bending[5] and CC ring	1101 vw			

stretching[3] in anthracene and 9-substituted anthracene				
		1085 w		CH bending out of phase in 9,10-dihydroanthracene[7], aliphatic CC stretching[13]
	1043 vw	1042 vs	1038	CH bending in plane in 9,10-dihydroanthracene[7], phenyl ring stretching + deformation in 9,10-dihydroanthracene[14], ortho-disubstituted benzene[8], internal tertiary carbon atom[8]
Aromatic CH in plane bending in anthracene[5]	1020 m	1016 mw	1024	Phenyl ring breathing in 9,10-dihydroanthracene[14]
Aromatic CH out of plane bending in anthracene[2], CC ring stretching + aliphatic CH out of plane wagging in 9-substituted anthracene[15]	985 vw	989 mw	996	CH out of plane bending in 9,10-dihydroanthracene[7]
Aromatic CH out of plane bending in anthracene and 9-substituted anthracene[3,5,6]	972 sh			
Aromatic CH out of plane bending[3,5] in anthracene and ring in plane bending[5] in 9-substituted anthracene	957 sh			
Aromatic CH out of plane bending in anthracene[5], CH_3 bending[6]	949 w	951-938 vw	950	CH out of plane bending in 9,10-dihydroanthracene[7]
Ring in plane bending[5,6] and aromatic CH out of plane bending[3,6] in 9-substituted anthracene	904 vw			
		898-888 m	890-885	Aliphatic CC stretching in dimers of anthracene derivatives,[16] skeletal bending in 9,10-dihydroanthracene[7]
Aromatic CH out of plane bending[5,6] of the group approximately perpendicular to the longer axis of the	879 w			

anthracene molecule (i.e. at the 10 position)[17]				
Aromatic CH out of plane bending in anthracene and 9-substituted anthracene[5,6]	866 w	869 vw		CH out of plane bending in 9,10-dihydroanthracene[7]
Aromatic CH out of plane bending in anthracene[5], CH_3 bending[6]	848 w	854 vw	851	CH out of plane bending in 9,10-dihydroanthracene[7]
Ring in plane bending in anthracene[5] and aromatic CH out of plane bending in 9-substituted anthracene[6], CH_2 bending[6,8]	834 w	832 w, sh		
Ring in plane bending in anthracene[5]	818 w	816 mw	820	Aliphatic CH out of plane bending in dianthracene[17]
aromatic CH out of plane bending[3] of the groups approximately parallel to the longer axis of the anthracene molecule (i.e. no 10 position)[17]	750 w	750 mw	760	CH out of plane bending in 9,10-dihydroanthracene[7] and ortho-disubstituted benzene[17]
aromatic CH out of plane bending in anthracene[5,17]; ring out of plane bending in 9-substituted anthracene[5,15]	733 w br			
Ring in plane bending in anthracene[2]	703 m	701 m	711	
Ring in plane bending in anthracene and 9-substituted anthracene[5,6]	693 m			
		685 m		Ring torsion in anthrone[13]
Ring in plane bending in anthracene[2,5]	637 vw	636-627 w	637	
Ring out of plane bending[3] and ring torsion[5] in anthracene	576 vw	571 w	584	Ring in plane bending in ortho-xylene[8,18]
Ring in plane bending in 9-substituted anthracene[6]	548 w	555 w	555	
Ring in plane bending in anthracene[2]	535 vw	528 w		Skeletal bending in 9,10-dihydroanthracene[7]
Ring in plane bending in	520 w	513 w	516	Phenyl out of phase bending in

anthracene[2,5]				9,10-dihydroanthracene[7]
Ring torsion[5,6], ring out of plane bending[3] in anthracene and 9-substituted anthracene	476 w			
		445 w		Ring deformation in ortho-xylene,[18] internal tertiary carbon atom[8]
Ring in plane bending in 9-methyl anthracene[8,18]	421 ms			
		406 m		Phenyl out of plane bending in 9,10-dihydroanthracene[7]
Ring bending in plane[2,5,6], ring torsion[6], in 9-methyl anthracene[8,18] **characteristic of fused benzene rings[12]**	**394 ms**			
Ring out of plane bending in anthracene[2]	366 w	365 m	361	Skeletal bending in 9,10-dihydroanthracene[7]
ring torsion in 9-substituted anthracene[6]	334 w	332 sh		
		326 s	327	CC deformation in dianthracene[1]
Ring torsion[5] and ring out of plane bending[3] in anthracene	237 w	242 w		Ring out of phase flapping in 9,10-dihydroanthracene[7]
Ring out of plane bending in anthracene[2], ring torsion in 9-substituted[6]	214 vw			
		153 vs		Lattice modes in dianthracene[1], central ring in plane bending in 9,10-dihydroanthracene[7]
Ring torsion in anthracene[5], CC bending in plane in 9-methyl anthracene[18]	148 w			
		137 vs	141	Lattice modes in dianthracene[1]
Ring torsion in anthracene and 9-substituted anthracene[5,6]	105 s	116 s	110	Lattice modes in dianthracene[1]
	74 vs	75 vs	71	Lattice modes in dianthracene[1]

v = very; w = weak; m = medium; s = strong; br = broad; sh = shoulder

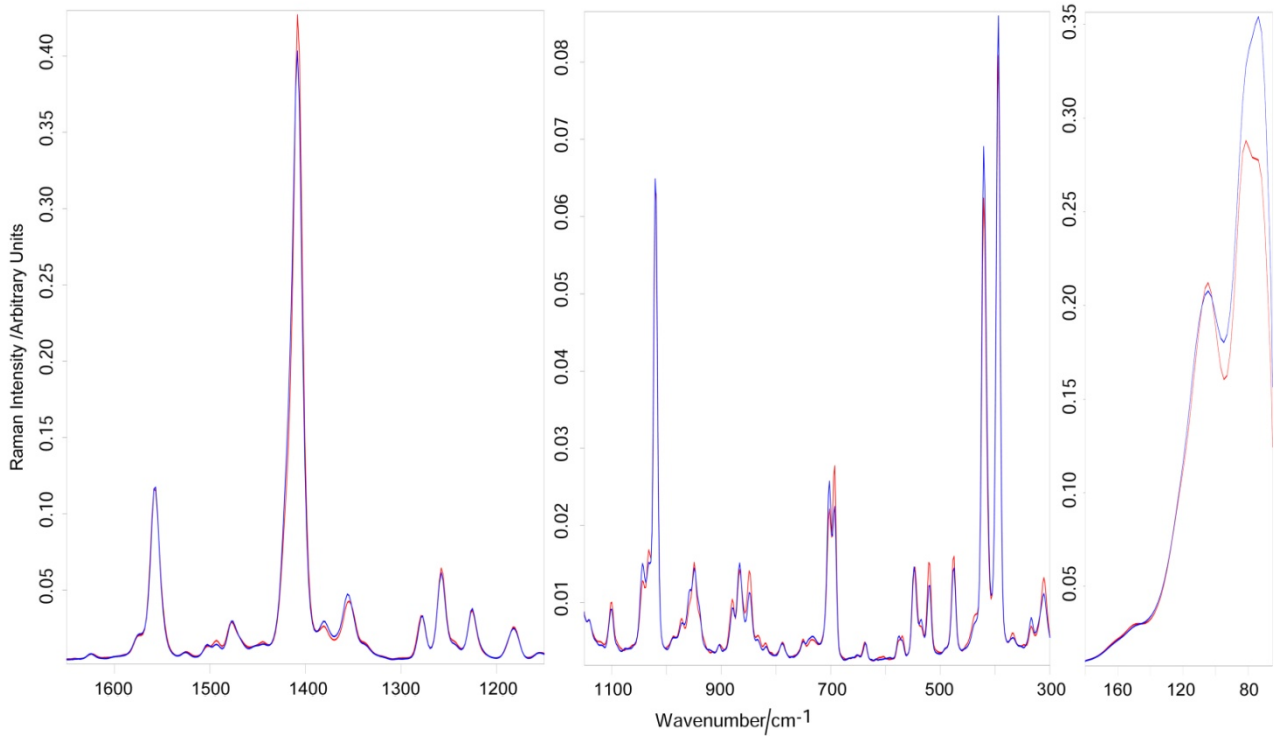

Fig. S7 Raman spectra of MAMA before (blue) and after irradiation (red).

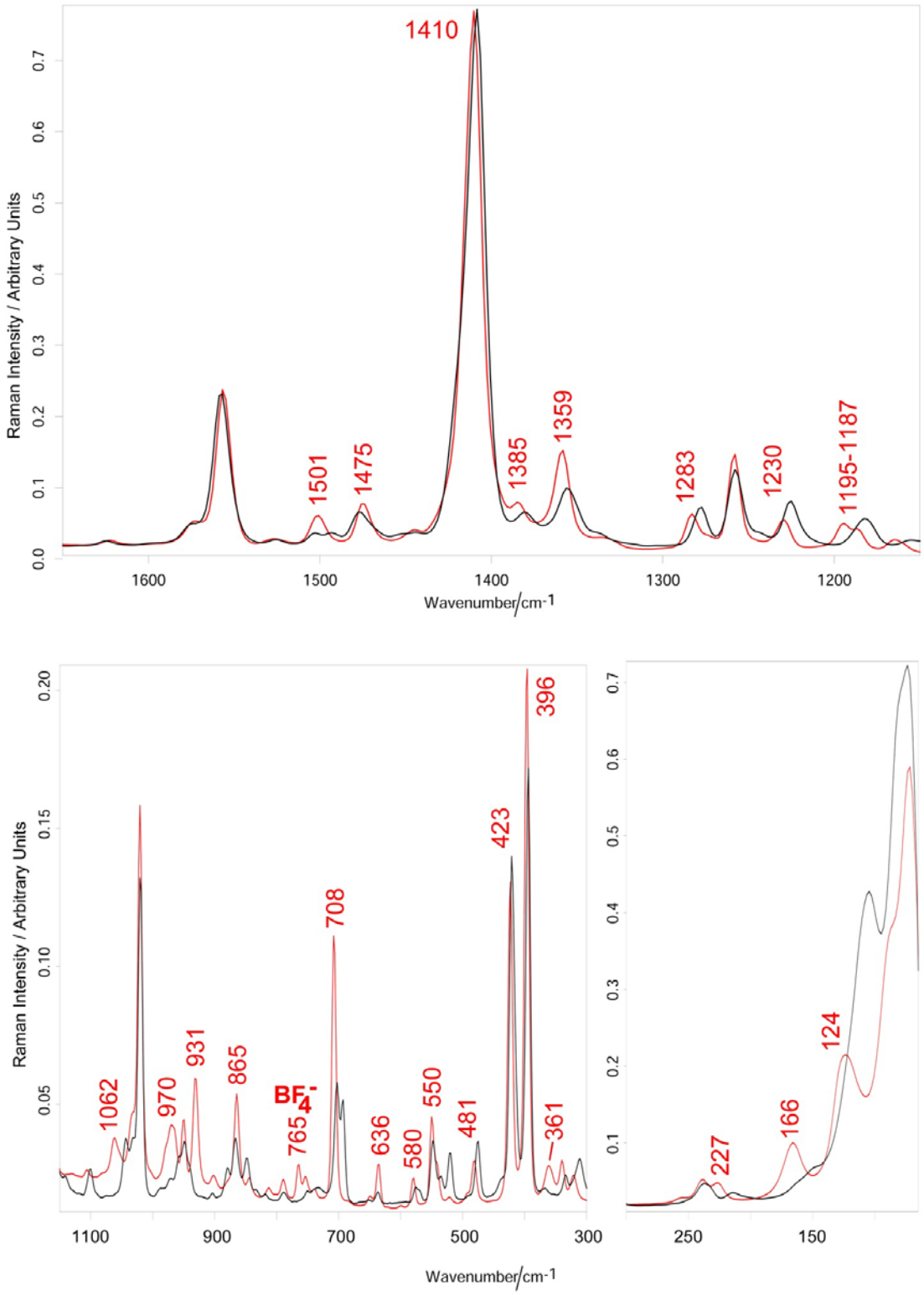

Fig. S8 Raman spectra of MAMA (black) and $[Ag(MAMA)_2][BF_4]$ (red). The band assignable to the BF_4^- ion has been indicated (765 cm^{-1}: FBF symmetric stretching).

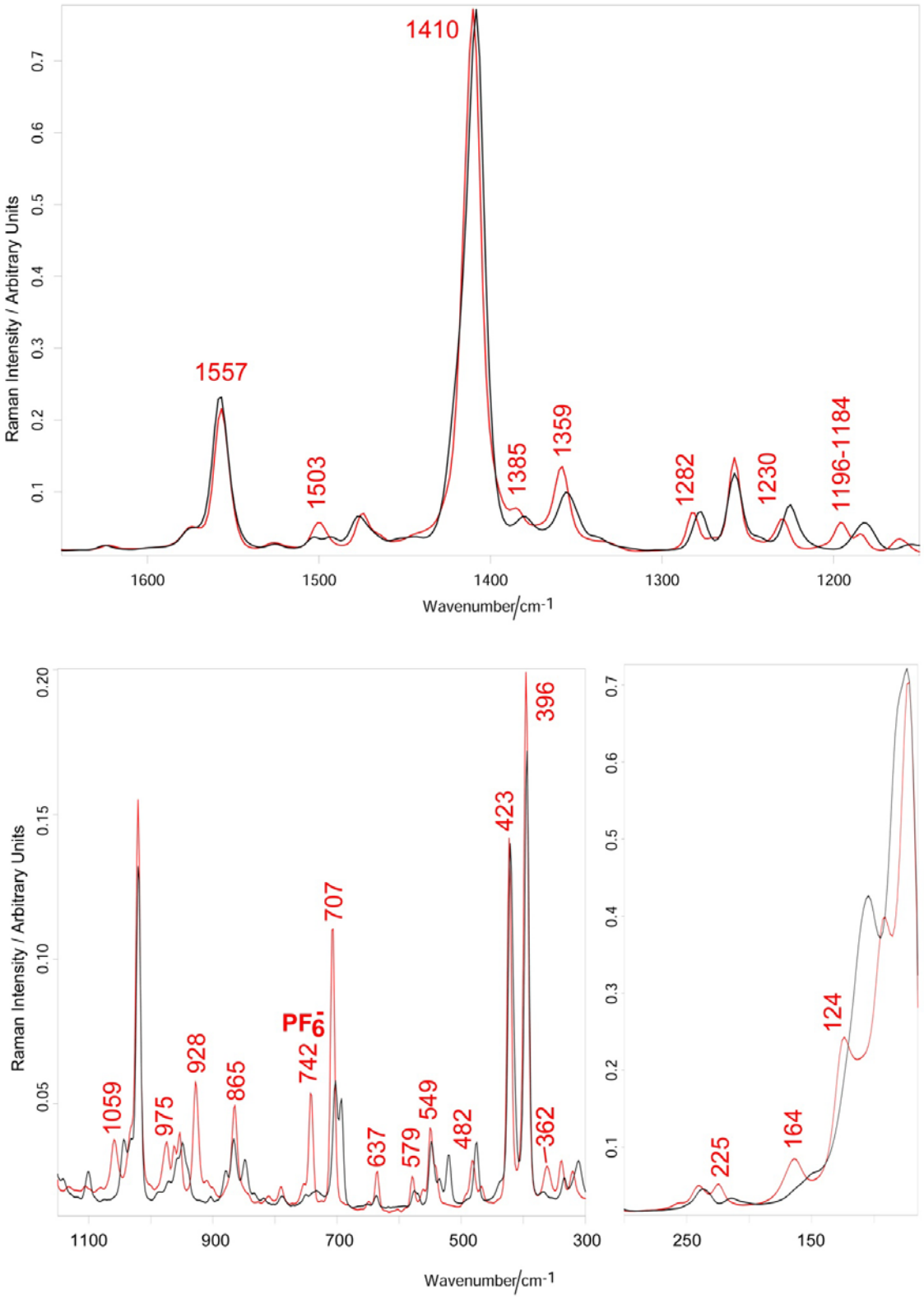

Fig. S9 Raman spectra of MAMA (black) and $[Ag(MAMA)_2][PF_6]$ (red). The band assignable to the PF_6^- ion has been indicated (742 cm^{-1}: FPF symmetric stretching).

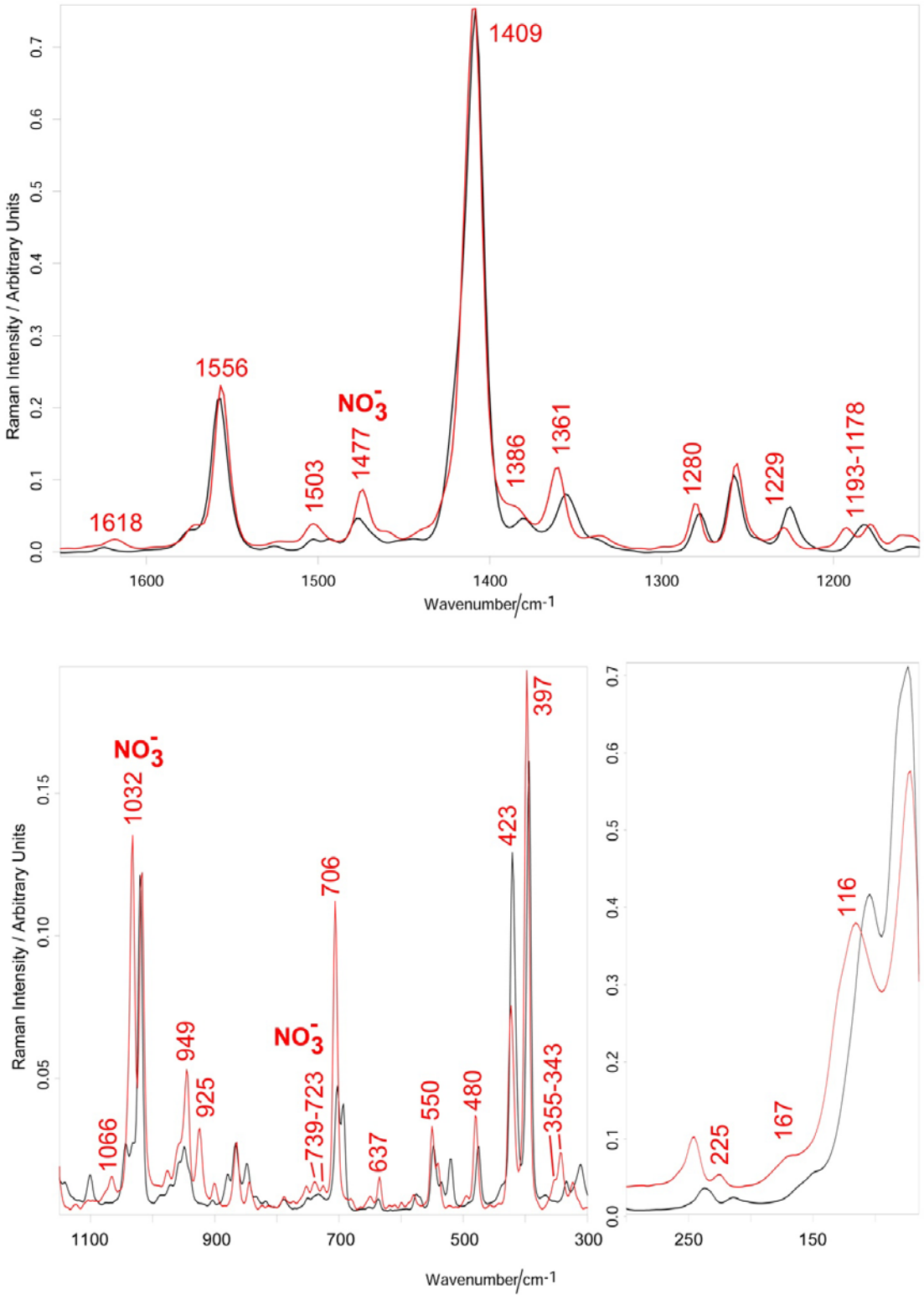

Fig. S10 Raman spectra of MAMA (black) and $[Ag(MAMA)_2][NO_3]$ (red). The bands assignable to the NO_3^- ion have been indicated (1477 cm^{-1}: N=O stretching in bidentate NO_3^- coordination; 1032 cm^{-1}: ONO symmetric stretching; 739-723 cm^{-1}: in plane NO_3^- deformation).

References

1. Y. Ebisuzaki, T. J. Taylor, J. T. Woo and M. Nicol, *J. Chem. Soc., Faraday Trans*, 1977, **73**, 253-264.
2. N. Abasbegović, N. Vukotić and L. Colombo, *J. Chem. Phys.*, 1964, **41**, 2575-2577.
3. J. Räsänen, F. Stenman and E. Penttinen, *Spectrochim. Acta A*, 1973, **29**, 395-403.
4. L.H. Colthup and S.E. Daly, Wiberley. Introduction to Infrared and Raman Spectroscopy. 3rd Edition, Academic Press, San Diego, 1990.
5. A. Alparone, V. Librando, *Spectrochim. Acta A*, 2012, **89**, 129– 136.
6. Y. S. Mary, H. T. Varghese, C. Y. Panicker, T. Thiemann, A. A. Al-Saadi, S. A. Popoola, C. Van Alsenoy and Y. A. Jasem, *Spectrochim. Acta A*, 2015, **150**, 533–542.
7. K. Morris and J. Laane, *J. Mol. Struct.*, 1997, **413-414**, 13-20.
8. F. R. Dollish, W. G. Fateley and F. F. Bentley, Characteristic Raman frequencies of organic compounds. Wiley-Interscience, Chichester, 1974.
9. K. S. Pitzer and D. W. Scott., *J. Am. Chem. Soc.*, 1943, **65**, 803-829.
10. W. F. Maddams, I. A. M. Royaud, *Spectrochim. Acta A*, 1990, **46**, 309-314.
11. M. Brigodiot and J. M. Lebas, *Spectrochim. Acta A*, 1971, **27**, 1325-1336.
12. I. L. Tocón, J. C. Otero, J. F. Arenas, J. V. Garcia-Ramos and S. Sanchez-Cortes, *Anal. Chem.*, 2011, **83**, 2518–2525.
13. Y. S. Mary, T. S. Yamuna, C. Y. Panicker, H. S. Yathirajan, M. S. Siddegowda, A. A. Al-Saadi, C. Van Alsenoy and J. Ahmad, *Spectrochim. Acta A*, 2015, **135**, 652–661.
14. M. Brigodiot and J. M. Lebas, *J. Mol. Struct.*, 1976, **32**, 297-309.
15. S. Kou, H. Zhou, G. Tang, R. Li, Y. Zhang, J. Zhao and C.i Wei, *Spectrochim. Acta A*, 2012, **96**, 768–775.
16. L. Opilik, P. Payamyar, J. Szczerbinski, A. P. Schütz, M. Servalli, T. Hungerland, A. D. Schlüter and R. Zenobi, *ACS Nano*, 2015, **9**, 4252–4259.
17. S. Singh and C. Sandorfy, *Can. J. Chem.*, 1969, **47**, 257-263.
18. M. Brigodiot and J. M. Lebas, *Spectrochim. Acta A*, 1971, **27**, 1315-1324.